Available online at www.sciencedirect.com
ScienceDirect
Ceramics International 35 (2009) 3427–3433
CERAMICS INTERNATIONAL
www.elsevier.com/locate/ceramint

Morphology and structure of YSZ powders: Comparison between xerogel and aerogel

Justine Fenech [a,*], Céline Viazzi [b], Jean-Pierre Bonino [a], Florence Ansart [a], Antoine Barnabé [a]

[a] University of Toulouse UPS-INP-CNRS, Institut Carnot CIRIMAT, 118 route de Narbonne, 31062 Toulouse cedex 09, France
[b] Saint-Gobain CREE, 550 avenue Alphonse Jauffret, BP 224, 84300 Cavaillon, France

Received 24 March 2009; received in revised form 18 May 2009; accepted 12 June 2009
Available online 7 July 2009

Abstract

Yttria-stabilized zirconia (YSZ) fine powders were prepared via sol–gel route in order to shape thermal barrier coatings (TBCs) from these powders. The main objective is to develop new undirectional coatings to allow best thermo-mechanical accommodations compared to conventional processes. To reach this aim, powders have to be able first to be highly dispersed into a sol (non-agglomeration, high specific surface area, etc.) and second to crystallize in the required metastable phase t′. Two routes have been used to dry gels: the conventional way which consists of simple evaporation of the solvent is compared to drying in supercritical conditions. Both YSZ powders after calcination at 950 °C of xerogel (Ex-xero-YSZ powder) and aerogel (Ex-aero-YSZ powder) crystallize in the tetragonal form. N_2 adsorption/desorption analysis of the Ex-xero-YSZ powder indicates an S_w of 2.8 m^2/g. For the Ex-aero-YSZ powder, the S_w (26 m^2/g) is much higher than of Ex-xero-YSZ, leading to a better sintering capability. This high S_w is correlated to the small crystallite size (26 nm) and the alveolar morphology of Ex-aero-YSZ powders compared to Ex-xero-powder (49 nm). By reducing particles size and increasing the S_w of the powders, supercritical drying appears as a promising way to prepare stable slurries or loaded sols from fine YSZ particles for TBC applications. Indeed, after preparing nanometric powders, they are dispersed into a sol before shaping on superalloys substrates. After thermal treatment at 950 °C for 2 h which corresponds to the working temperature of TBC, the final aim will be to prepare ceramic YSZ coatings.

Keywords: A. Drying; B. X-ray methods; D. ZrO_2; Microstructure

1. Introduction

Zirconia materials are largely used for various applications. Particularly, yttria stabilized zirconium (YSZ) oxide presents great interest for thermal barrier coatings (TBCs) which act as thermal insulating layers on superalloys in aircraft engines. These TBCs are synthesized either by electron beam physical vapor deposition (EB-PVD) [1] or by plasma spray (PS) process [2], giving rise to columnar and lamellar microstructures respectively. To develop TBCs with a non-directional porosity, these two physical processes cannot be used. Few research works dealing with this problematic issue have been reported, except those of Viazzi et al. [3,4]. The authors presented a sol–gel route combined with a dip-coating process as an alternative technique to the two mentioned above, to shape, from a composite sol, thick layers on nickel-based superalloys. In this work, the final objective is not to fill the voids of plasma spray TBCs but to replace the conventional process by an innovative technology based on sol–gel route. A previous study has been performed to optimize the temperature profiles (dwell temperature at 950 °C (working temperature) for 2 h). The formulation of stable slurries (or composite sols) and the perfect covering of the rough substrate surfaces demand control of several parameters: not only are the sol parameters (viscosity, concentration of the powder) important, the powder characteristics with respect to their granulometry, structure and morphology must also be controlled. In particular, we strongly need to have thin particles. Consequently, this research focuses on the drying method of the gel since it is well known that this influences the morphological characteristics of the resulting oxide.

Numerous papers study how the different control parameters during the synthesis of zirconium gels can have an influence on the crystallization, phase transition and sintering [5–8].

* Corresponding author. Tel.: +33 05 61 55 62 84; fax: +33 05 61 55 61 63.
E-mail address: fenech@chimie.ups-tlse.fr (J. Fenech).

0272-8842/$36.00
doi:10.1016/j.ceramint.2009.06.014

When zirconia powders (YSZ) are prepared using the sol–gel route [9–14] drying is mainly governed by the capillary pressure. Conventional drying consists of drying the gel at ambient temperature in an oven to remove the liquid phase (alcohol and water from the sol–gel synthesis) from the porous structure [6]. Parallel to this, supercritical drying offers the advantage of keeping the gel structure before the drying step by controlling the critical temperature and pressure of the liquid to be removed from the pores [15]. Two supercritical drying methods exist: high temperature and low temperature methods. The second method is an alternative to the first one, which consists of replacing the solvent originally present in the gel with a liquid whose critical point is close to ambient temperature. The fluid commonly used for this process is liquid CO_2, with a low critical temperature (less than 40 °C) and moderate pressure (less than 80 bars) [16,17].

The aim of this paper is not to work on the chemistry of the sol–gel synthesis but to use the as-prepared powders for shaping into specific thermal barrier coating applications after thermal treatment at 950 °C. The shaping aspect will be discussed in another paper. Hence, the main goal here is to compare the structural and morphological properties of YSZ powders using two drying techniques: conventional and high temperature supercritical drying.

To facilitate this study, X-ray analysis and Rietveld refinement have been performed to determine the crystallographic properties of the YSZ powders synthesized via sol–gel route. The average size of the crystallites has been estimated for the two kinds of powder using the Scherrer formula. In addition, the surface specific area of heat-treated YSZ oxide powders has been measured using the Brunauer–Emmett–Tellet (BET) method. By correlation with scanning electron microscopy (SEM) results, morphological investigation has been made for a better understanding of the influence of such drying method on the final YSZ oxide powders. Finally, laser granulometry measurements have been performed to study if the supercritical drying process is able to limit sintering during heat treatment. A consequence is to promote the grinding step to obtain smaller particles than those from the traditional drying method.

2. Experimental

2.1. Synthesis of YSZ powders by the sol–gel route

2.1.1. Synthesis

Zirconia precursor gels with 9.7 mol.% yttrium were prepared by the sol–gel route using zirconium (IV) propoxide ($ZrO(Pr)_4$) (Aldrich), yttrium (III) nitrates hexahydrate (Acros Organics), 1-propanol (solvent), acetylacetone (AcAc) and water. The order of introduction the different reagents in the mixture is presented in the flow chart in Fig. 1a. Due to the hygroscopic properties of zirconium propoxide, acetylacetone was first introduced to 1-propanol as a complexing agent in order to prevent any uncontrolled reactions between the alkoxide and water. Furthermore, all syntheses were performed under argon atmosphere in order to avoid the problem of fast hydrolysis of alkoxide by water. The molar ratios [AcAc]/[$Zr(OPr)_4$] and [H_2O]/[$Zr(OPr)_4$] are 0.7 and 8.5 respectively and the zirconium propoxide concentration is kept constant at 0.5 mol/L. The gelation, hydrolysis and condensation reactions were carried out at room temperature in ambient atmosphere. YSZ precursor sols are mechanically stirred for half an hour after synthesis.

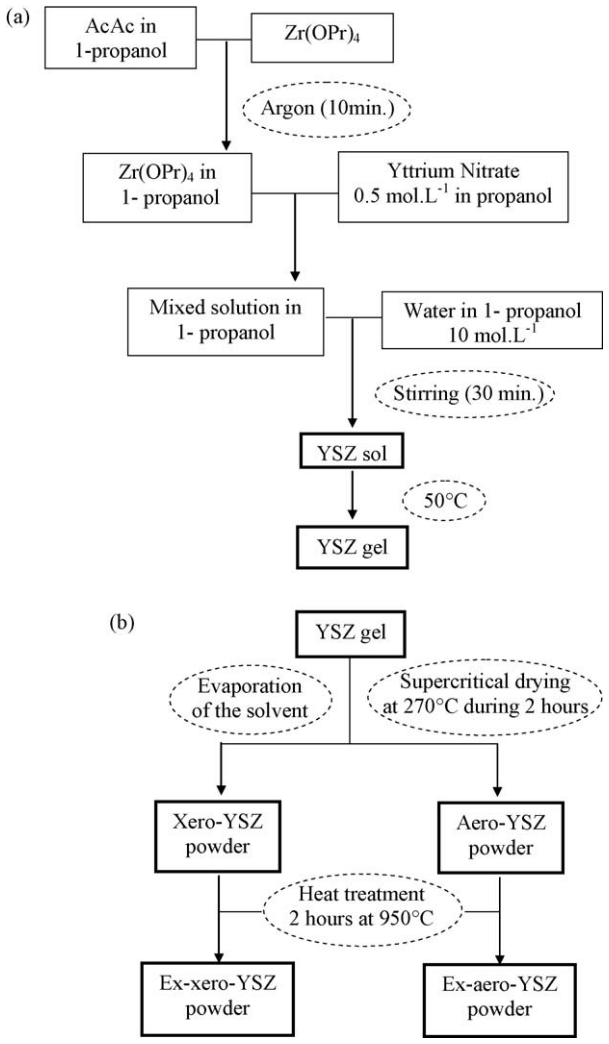

Fig. 1. (a) Procedure for sol–gel synthesis; (b) procedures for drying zirconia gel.

2.1.2. Drying methods of YSZ precursor gels

The resulting sols, heated at 50 °C in a drying oven, became bright monolith gels which are free of precipitates, after a few hours (about 4 h or 5 h). Two methods for drying the zirconia precursor gels were studied (Fig. 1b). The first one is the traditional way, which consists of drying the gels in an oven by simple evaporation of the solvent. The resulting products are dried gels or xerogels (referred to as Xero-YSZ powder). The second method is the supercritical drying of fluids, leading to the production of zirconia aerogel whose structure is similar to the wet gel. After sol/gel transition, the gel is transferred to a stainless steel autoclave (Parr Instrument, 160 mL) equipped with a temperature and pressure regulator. By heating at

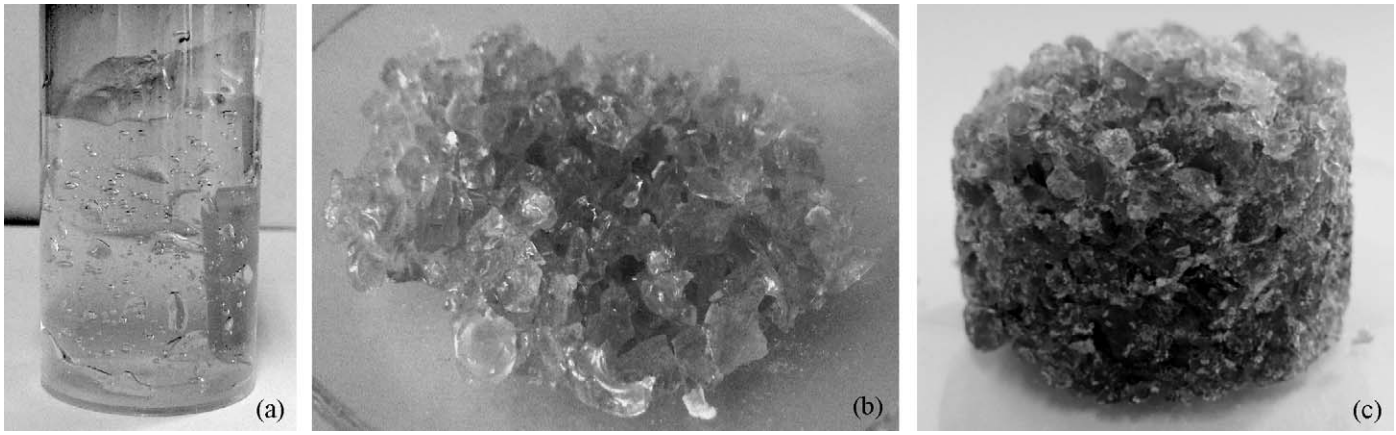

Fig. 2. Photographs: (a) YSZ wet gel; (b) X-YSZ; (c) A-YS(b).

270 °C, the temperature and pressure in the autoclave reach the critical conditions of the propanol (T_c = 263 °C; P_c = 51 bar). Temperature is kept constant at 270 °C for 2 h; during the last hour of heating, the solvent is slowly released and then the reactor is cooled to room temperature. A zirconia monolith aerogel is obtained (referred to as Aero-YSZ powder), which is brown in colour due to the presence of residual organic compounds (Figs. 2 and 3).

2.1.3. Annealing

After the drying process, both the Xero-YSZ powder and Aero-YSZ powder are calcined at 950 °C for 2 h in the same furnace (heating rate: 100 °C/h) in order to obtain crystallized white zirconia powders. Henceforth, YSZ powder obtained from the calcination of the xerogel will be called Ex-xero-YSZ powder; and the oxide powder obtained from the calcination of the aerogel will be called Ex-aero-YSZ powder.

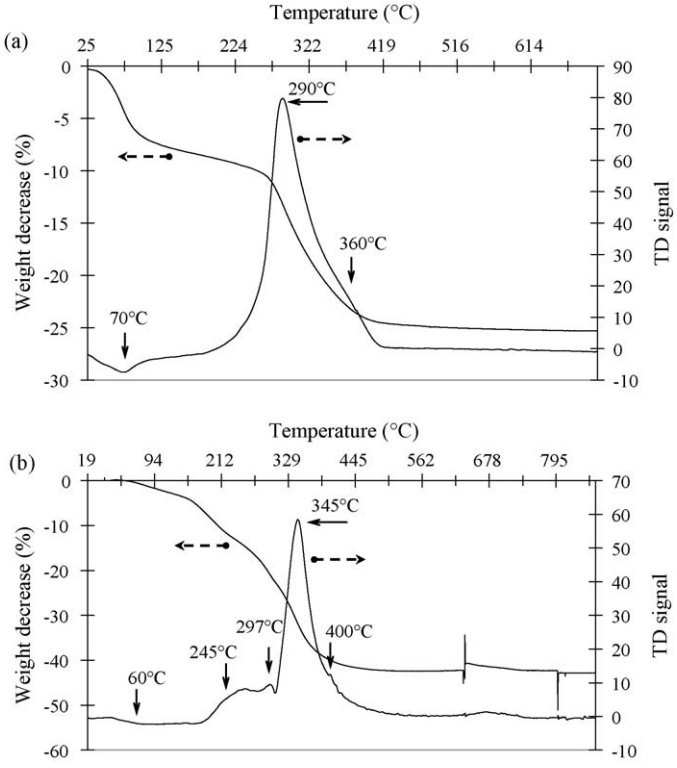

Fig. 3. Thermal analysis (TG/DTA) profile of: (a) Aero-YSZ zirconia aerogel obtained after supercritical drying in 1-propanol; (b) Xero-YSZ obtained after conventional drying.

2.2. Characterisation methods

2.2.1. Structural analysis by XRD

Structural analyses of the Ex-xero-YSZ and Ex-aero-YSZ powders were performed with X-ray diffraction measurements coupled with Rietveld refinement. The patterns were measured at room temperature with a Brucker AXS D4 diffractometer. Copper radiation was used as the X-ray source ($\lambda(CuK_{\alpha 1})$ = 1.5406 Å; $\lambda(CuK_{\alpha 2})$ = 1.5445 Å) and filtered with Ni filter. The average crystallite size of the particles, assimilated to the size of the diffracting domains, was calculated by the Scherrer formula: $d = 0.9\,\lambda/\mathrm{FWHM}\,\cos\theta$ where λ = 0.15405 nm; FWHM is the full width at half maximum of the peaks after correction for the instrumental contribution; and θ is the diffraction angle. For this calculation, it is assumed that there is no microstrains.

Thermo gravimetric (*TG*) *and differential thermal* (*DT*) *analyses* were performed on A-YSZ sample using a SETARAM 92-16-8 apparatus in air flow, using Pt reference and with a heating rate of 3 °C/min.

2.2.2. Measurement of the specific area by BET (Brunauer–Emmett–Teller) method

The specific surface areas of the powders calcined at 950 °C were determined by the BET method using the N_2 adsorption–desorption at 77 K. The powders were first degassed at 250 °C for 40 min before nitrogen adsorption. The powders were mechanically ground for 10 min before the BET measurement.

2.2.3. Microstructural analysis

The microstructure of the oxide powders was observed with scanning electron microscopy using a field emission gun (SEM–FEG) *Jeol-6700F*. The agglomeration state of the powders was analysed using laser granulometry (*Coulter LS 100Q*) and particle size distribution of the samples was recorded.

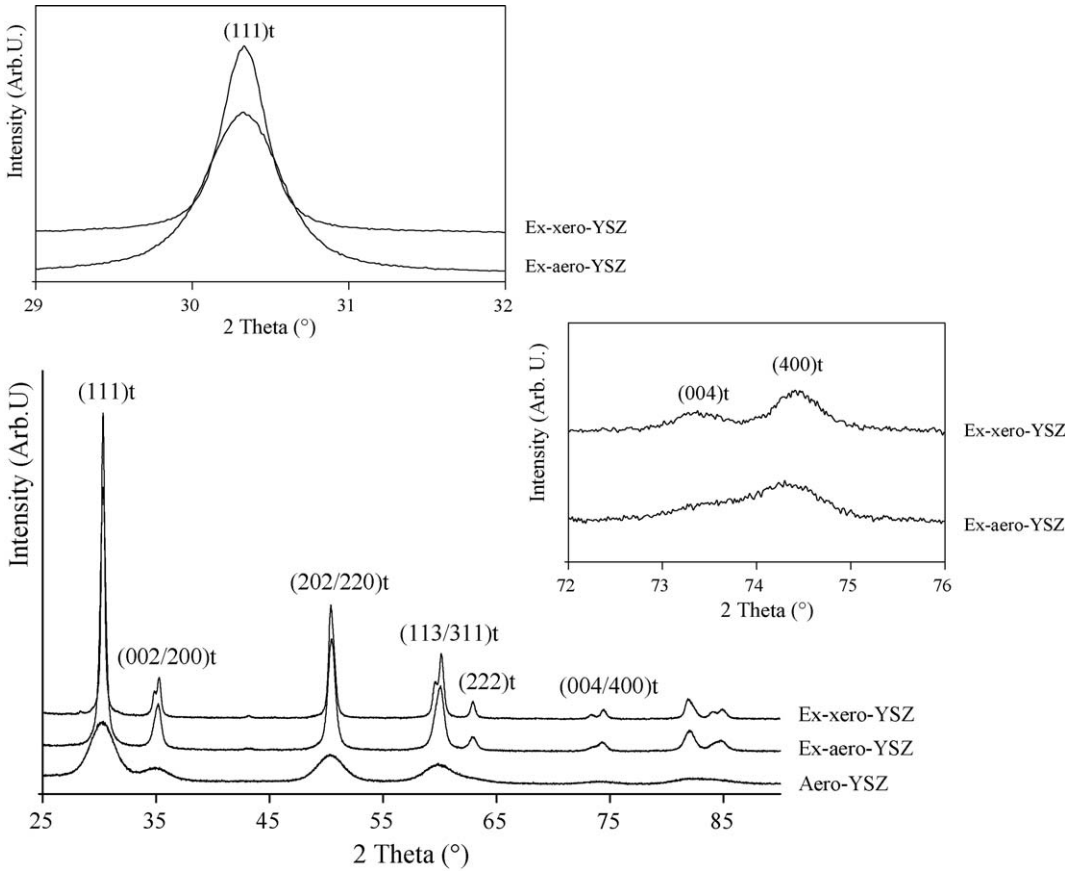

Fig. 4. X-Ray diffraction patterns of Aero-YSZ (after drying at 270 °C), Ex-aero-YSZ and Ex-xero-YSZ powders after heat treatment at 950 °C. Inset: zooms at 29°–32° and 72°–76° angular domains show the evolution of broadening of the diffraction peaks with respect to the drying process.

3. Results and discussion

3.1. Specific characterisation—structural analysis by XRD and estimated crystallite size

Before structural characterisation, thermogravimetric (TG) measurements have been carried out in order to characterise the aerogel. The TG diagram of Aero-YSZ in Fig. 3a presents three weight decreases at around 70 °C, 195 °C and 290 °C. The first weight loss (7%) is associated with the broad endothermic DTA peak. It is attributed to the desorption of physisorbed species related to the loss of water. A second mass loss centered at 290 °C is highly exothermic and combined with the higher weight loss of 16%. It is probably due to the combustion of covalently anchored alkoxy groups over the surface of the sample. The last one (360 °C) is attributed to the first step of germination [18]. As for the Ex-xero-YSZ powder (Fig. 3b), three exothermic peaks at 245 °C, 297 °C and 345 °C (major intensity) are due to the degradation of different organic compounds used in the synthesis of the YSZ sol. In addition, zirconia crystallization seems to be slightly shifted toward a higher temperature (400 °C) compared to Ex-aero-YSZ powder (360 °C).

The Ex-xero-YSZ and Ex-aero-YSZ powders were analysed using X-ray diffraction before and after calcination at 950 °C for 2 h. The Xero-YSZ sample is amorphous whereas Ex-xero-YSZ is crystallized. In fact, according to the X-ray diffraction patterns (Fig. 4) and Rietveld analysis, we found that the Ex-xero-YSZ powder exhibits a tetragonal symmetry (space group: $P4_2/nmc$). Ex-aero-YSZ also has this symmetry but it is less visible in the X-ray diffraction pattern due to the low $c/a\sqrt{2}$ ratio (see Table 1) and peak broadening, indicating a decrease in the crystallite size (insets Fig. 4). The XRD pattern relative to Aero-YSZ is characteristic of the crystallization of zirconium precursors. It can be seen that the diffraction peaks, albeit broad, are centered on the position corresponding to the interreticular distances of zirconia tetragonal phase. After heat treatment at 950 °C for 2 h, Ex-aero-YSZ preserves its tetragonal form. On the other hand, the diffraction peaks for the zirconia powder are narrower which indicates the growth of the crystallites.

Previous studies showed that the evolution of the tetragonality ($c/a\sqrt{2}$) of the sol–gel powders versus the amount

Table 1
Structural parameters of the YSZ powders after heat treatment at 950 °C. t′ indicates the presence of tetragonal metastable phase.

	Structure	Lattice parameters (nm)			d (nm)
		a	c	$c/a\sqrt{2}$	
Ex-xero-YSZ	t′	0.36129(5)	0.5162(2)	1.0101(6)	49
Ex-aero-YSZ	t′	0.36143(5)	0.5161(2)	1.0097(5)	26

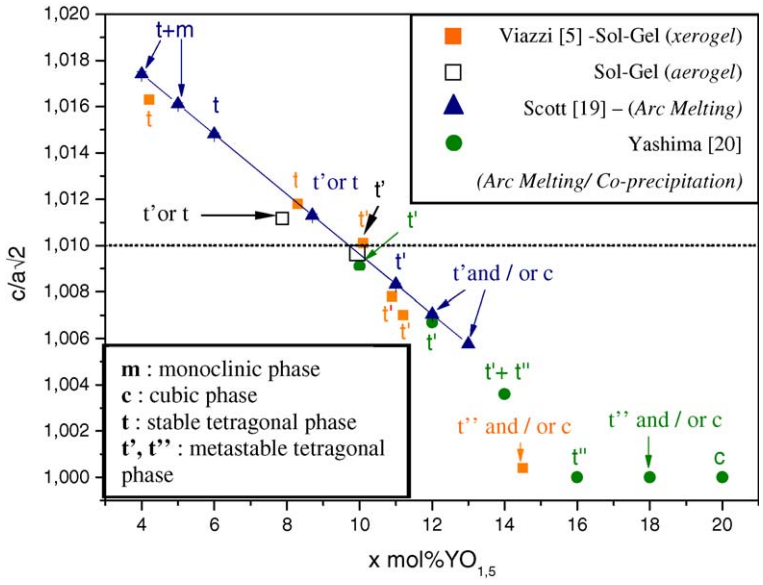

Fig. 5. Comparison of the tetragonality of powders obtained by the sol–gel route and the results reported in the literature.

of yttria [5] was in good agreement with results obtained by Scott [19] and Yashima et al. [20] using other synthesis methods. In this case, the sol–gel powders were Ex-xero-YSZ powders with 4.5–13 mol.% $YO_{1.5}$. It has been observed that whatever the method used to synthesize the YSZ powder, the tetragonal character ($c/a\sqrt{2}$) decreases when the amount of yttrium increases (Fig. 5). Tetragonality for Ex-aero-YSZ with 8% and 9.7% molar $YO_{1.5}$ is respectively 1.0117(2) and 1.0097(5) as calculated by Rietveld refinement. The graph in Fig. 5 shows that the sol–gel route combined with supercritical drying makes it possible to synthesize metastable tetragonal powders (t′ phase) [19] with the $c/a\sqrt{2}$ ratio tending to 1.010. To sum up this study on the structural analysis, the average size of the crystallites determined using the Scherrer formula (Table 1) shows that the Ex-aero-YSZ crystallites (26 nm) are almost two times smaller than the Ex-xero-YSZ crystallites (49 nm). These results are well correlated with the microscopic analyses.

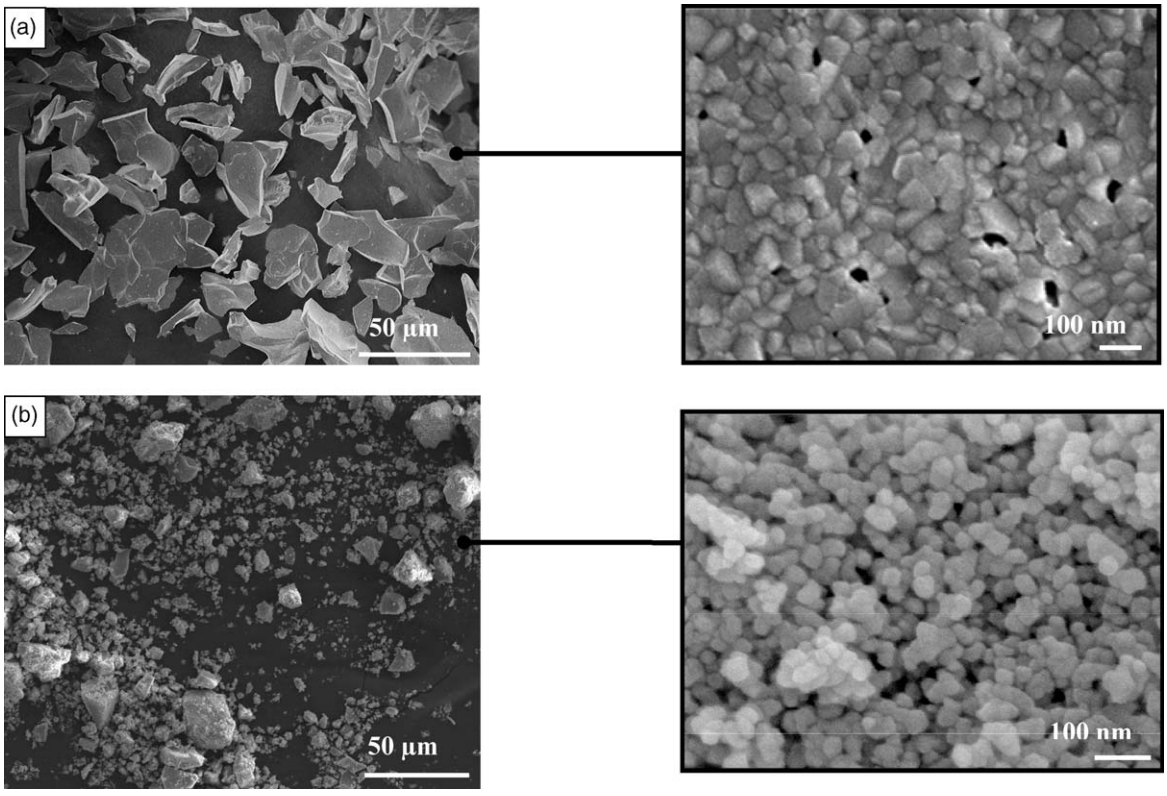

Fig. 6. Influence of the drying technique on the final microstructure of YSZ powders calcined at 950 °C: (a) Ex-xero-YSZ; (b) Ex-aero-YSZ.

3.2. Microscopical characterisation

Fig. 6 shows the typical microstructure of Ex-xero-YSZ and Ex-aero-YSZ after calcinations at 950 °C for 2 h. Upon magnification, the two powders have quite different microstructure in spite of having undergone similar thermal treatment. Ex-xero-YSZ consists of very well-defined grains. Their coalescence, as well as densification and reduced porosity are noted and have to be attributed to better sintering capability of such primary grains at 950 °C. On the contrary, the microstructure of the Ex-aero-YSZ powder is more porous, and as a result, sintering is drastically reduced. The correlation between the XRD analysis and the microscopic observation demonstrates that both Ex-xero-YSZ and Ex-aero-YSZ are monocrystalline particles but that of Ex-aero-YSZ are finer. In addition, the specific surface area (BET) of YSZ powders calcined at 950 °C are 2.8 m^2/g for Ex-xero-YSZ and 26 m^2/g for Ex-aero-YSZ from N_2 isotherms at 77 K. These values are in good agreement with the previous microscopic characterization: a porous structure and an alveolar morphology for the Ex-aero-YSZ powder resulting in the agglomeration of very fine particles.

The aim of the next study is to compare the behaviour of the two YSZ powders under identical grinding treatment. The influence of the drying process on the granulometry of Ex-xero-YSZ and Ex-aero-YSZ will be discussed. For this study, all powders have been mechanically grinded for 10 min.

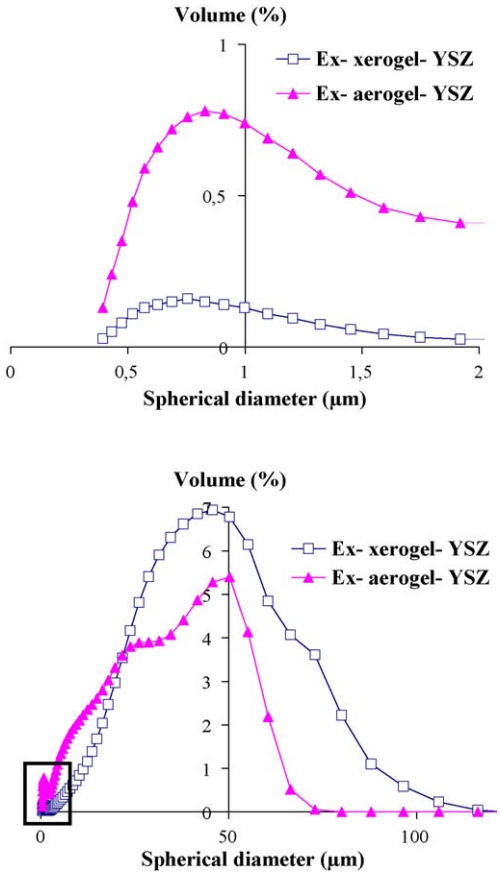

Fig. 7. Granulometric distribution of the Ex-xero-YSZ and Ex-aero-YSZ samples mechanically ground for 10 min.

Table 2
Granulometric dispersion of the Ex-xero-YSZ and Ex-aero-YSZ samples mechanically ground for 10 min.

	D10	D25	D50	D75	D90
Ex-xero-YSZ	15 µm	25 µm	34 µm	55 µm	73 µm
Ex-aerogel-YSZ	3 µm	8 µm	22 µm	41 µm	55 µm

3.3. Grinding behaviour of YSZ powders according to the drying process

In Fig. 7, the granulometric distribution measurements clearly indicate that after grinding, the resulting particles are agglomerates constituted of the finest particles described in the previous paragraphs, i.e. monocrystalline particles of Ex-Xerogel-YSZ (49 nm) and Ex-YSZ-aerogel (26 nm). The granulometric distribution is narrower for Ex-aero-YSZ than for Ex-xero-YSZ. For the Ex-xero-YSZ powder, the granulometric distribution is trimodal with the average spherical diameters of 0.8 µm, 50 µm and 75 µm. The ex-aero-YSZ powder Exhibits 4 particles size with the average spherical diameters of 0.8 µm, 12.5 µm, 25 µm and 50 µm, which is less important than for Ex-xero-YSZ. Furthermore, as it can be seen in Fig. 7, the Ex-aero-YSZ modes are clearly shifted toward the smaller spherical diameters compared to the Ex-xero-YSZ. The narrowing of granulometric distribution for Ex-aero-YSZ can be verified if we focus in Table 2 shows the evolution of diameters with D10, D25, D50, D75 and D90, which represents 10 vol.%, 25 vol.%, 50 vol.%, 75 vol.%, 90 vol.% of particle distribution respectively. To conclude, it is notable that with an equal grinding time, the granulometric analysis of Ex-xero-YSZ and Ex-aero-YSZ powders differs significantly in terms of the number of the granulometric modes and the width of the average spherical diameter of the particles.

4. Conclusions

YSZ powders synthesized via sol–gel process combined with conventional or supercritical drying of the wet gel have been studied. Both samples crystallize in the tetragonal form at 950 °C. Their tetragonalities are very close and indicate that the sol–gel process enables formation of the tetragonal metastable (t′) solid solution for 9.7 mol.%$YO_{1.5}$. After the autoclave treatment using supercritical drying method, the zirconia aerogel is already crystallized in the tetragonal form whereas after the traditional drying process the zirconia xerogel is amorphous. The choice of drying methods of the gels is a critical step to obtain different powder morphologies. While the Ex-xero-YSZ powder exhibits a densified structure (S_w = 2.8 m^2/g) of agglomerates constituted by 50 nm crystallites, the Ex-aero-YSZ powder presents a more porous structure (S_w = 26 m^2/g) with elementary crystallites (26 nm). It is clear that due to its alveolar structure, the grinding behaviour of an aerogel after calcination at 950 °C is better than for a xerogel.

For this grinding condition, the granulometric distribution of Ex-aero-YSZ powder is narrower than for Ex-xero-YSZ and shifted to the smaller particles size. These results are very promising for the preparation of stable suspensions of fine YSZ particles to shape the powders in chemical process.

Acknowledgment

The authors would like to thank the French DGA and CNRS for their financial support (DGA-CNRS grant).

References

[1] F. Crabos, PhD Thesis, Institut National Polytechnique de Toulouse, 96 INPT0092, France, 1996.
[2] R. Mevrel, C. Rio, M. Poulain, C. Diot, F. Nardou, Technical Report No.28/2019M, ONERA, 1987.
[3] C. Viazzi, J.P. Bonino, F. Ansart, Synthesis by sol–gel route and characterization of yttria stabilized zirconium coatings for thermal barrier applications, Surf. Coat. Technol. 201 (2006) 3889–3893.
[4] C. Viazzi, R. Wellman, D. Oquab, J. Nicholls, D. Monceau, J.P. Bonino, F. Ansart, in: Proceedings of the 7th International Symposium on High Temperature Corrosion and Protection of Materials, Les Embiez, (2008), p. 21.
[5] C. Viazzi, J.-P. Bonino, F. Ansart, A. Barnabé, Structural study of metastable tetragonal YSZ powders produced via a sol–gel route, J. Alloy Compd. 452 (2008) 377–383.
[6] C. Viazzi, A. Deboni, J.Z. Ferreira, J.P. Bonino, F. Ansart, Synthesis of YSZ by sol–gel route influence of experimental parameters and large scale production, Solid State Sci. 8 (2006) 1023–1028.
[7] P. Colomban, Gel technology in ceramics, glass-ceramics and ceramic–ceramic composites, Ceram. Int. 15 (1989) 23–50.
[8] P. Colomban, E. Bruneton, Influence of hydrolysis conditions on crystallization, phase transitions and sintering of zirconia gels prepared by alkoxide hydrolysis. Advanced materials from gels, J. Non-Cryst. Sol. 201 (1992) 147–148.
[9] Q. Sun, Y. Zhang, J. Deng, S. Chen, D. Wu, A novel preparation process for thermally stable ultrafine tetragonal zirconia aerogel, Appl. Catal. 152 (1997) L165–L171.
[10] Y. Huang, B. Zhao, Y. Xie, Preparation of zirconia-based acid catalysts from zirconia aerogel of tetragonal phase, Appl. Catal. 172 (1998) 327–331.
[11] Y. Cao, J. Hu, Z. Hong, J. Deng, K. Fan, Characterization of high-surface-area zirconium aerogel synthesized from combined alcohothermal and supercritical fluid drying techniques, Catal. Lett. 81 (2002) 107–112.
[12] Z.G. Wu, Y.X. Zhang, L.P. Xu, D.S. Liu, Preparation of zirconium aerogel by heating of alcohol–aqueous salt solution, J. Non-Cryst. Sol. 330 (2003) 274–277.
[13] A. Lecomte, F. Blanchard, A. Dauger, M.C. Silva, R. Guinebretière, Synthesis and sintering of zirconium oxide aerogel, J. Non-Cryst. Sol. 225 (1998) 120–124.
[14] D. Suh, T. Park, Synthesis of high-surface-area zirconia aerogels with a well-developed mesoporous texture using CO_2 supercritical drying, Chem. Mater. 14 (2002) 1452–1454.
[15] A.C. Pierre, G.M. Pajouk, Chemistry of aerogels and their applications, Chem. Rev. 102 (2002) 4243.
[16] C.N. Chervin, B.J. Clapsaddle, H. Chiu, A.E. Gash, J.H. Satcher, S.M. Kauzlarich, Aerogel synthesis of yttria-stabilized zirconium by a non-alkoxide sol–gel route, Chem. Mater. 17 (2005) 3345–3351.
[17] Z. Zhao, D. Chen, X. Jiao, Zirconium aerogels with high surface area derived from sols prepared by electrolyzing zirconium oxychloride solution: comparison of aerogels prepared by freeze-drying and supercritical CO_2(l) extraction, J. Phys. Chem. Coat. 111 (2007) 18738–18743.
[18] C. Laberty-Robert, F. Ansart, C. Deloget, M. Gaudon, A. Rousset, Powder synthesis of nanocrystalline ZrO_2–8%Y_2O_3 via a polymerization route, Mater. Res. Bull. 36 (2001) 2083–2101.
[19] H.G. Scott, Phase relationships in the zirconium–yttria system, J. Mater. Sci. 10 (1975) 1527.
[20] M. Yashima, M. Kakihana, M. Yoshimura, Metastable-stable diagrams in the zirconium containing systems utilized in solid-oxide fuel cell application, Solid State Ionics 86 (1996) 1131.